nature structural & molecular biology

The chromatin-remodeling enzyme ACF is an ATP-dependent DNA length sensor that regulates nucleosome spacing

Janet G Yang[1,2], Tina Shahian Madrid[1,2], Elena Sevastopoulos[1] & Geeta J Narlikar[1]

Arrays of regularly spaced nucleosomes directly correlate with closed chromatin structures at silenced loci. The ATP-dependent chromatin-assembly factor (ACF) generates such arrays *in vitro* and is required for transcriptional silencing *in vivo*. A key unresolved question is how ACF 'measures' equal spacing between nucleosomes. We show that ACF senses flanking DNA length and transduces length information in an ATP-dependent manner to regulate the rate of nucleosome movement. Using fluorescence resonance energy transfer to follow nucleosome movement, we find that ACF can rapidly sample DNA on either side of a nucleosome and moves the longer flanking DNA across the nucleosome faster than the shorter flanking DNA. This generates a dynamic equilibrium in which nucleosomes having equal DNA on either side accumulate. Our results indicate that ACF generates the characteristic 50- to 60-base-pair internucleosomal spacing in silent chromatin by kinetically discriminating against shorter linker DNAs.

It has been known for almost 30 years that transcriptionally silent chromatin consists of long stretches of regularly spaced nucleosomes[1–3]. ACF has been shown to be the major enzyme responsible for generating these structures in higher eukaryotes[3,4]. Yet how ACF generates these structures, and how it does so at multiple locations with varying DNA sequences, is not known.

ACF is part of the ISWI family of chromatin-remodeling complexes. ISWI-family complexes are generally involved in regulation of transcription, often in transcriptional repression[3,5–9]. Substantial previous work has shown that ISWI complexes translationally reposition nucleosomes along DNA using ATP[10–12]. Several of the ISWI-family complexes can generate regularly spaced arrays of nucleosomes[3,4,13,14]. All ISWI-family complexes have a central ATPase subunit that is homologous to the *Drosophila melanogaster* ISWI protein, along with a variable number of additional subunits[4,9,13–17]. Human ACF contains the ATPase subunit SNF2h and a noncatalytic subunit, ACF1 (refs. 16,18,19). Notably, the ATPase subunit of ISWI complexes alone is capable of moving nucleosomes and the outcome of its activity is modulated by the noncatalytic subunits[10–12,20–22].

The ability of ACF to generate arrays with evenly spaced nucleosomes raises the key question of how ACF compares and equalizes the linker DNA on either side of a nucleosome. The nucleosome-spacing activity of ACF is directly related to its ability to move a mononucleosome to the center of a short stretch of DNA[3,4,11,12]. Here, we have used mononucleosome centering as a model system to understand how human ACF spaces nucleosomes. We follow the movement of nucleosomes in real time by using fluorescence resonance energy transfer (FRET) and show that the length of flanking DNA regulates the ATPase activity of human ACF and the rate of movement of DNA across the histone octamer. This generates a dynamic equilibrium of nucleosome positions in which the centrally located positions predominate. Our results also help explain how the noncatalytic subunit ACF1 may modulate the activity of the ATPase subunit SNF2h.

RESULTS

ACF but not SNF2h appears to center nucleosomes

Previous work with ACF has shown that whereas ACF can center nucleosomes, the ATPase subunit alone cannot[11,21]. To confirm that our human ACF preparation behaves analogously, we first compared the mononucleosome-centering ability of ACF and that of SNF2h alone using a conventional gel-based method. Mononucleosomes were positioned at the end or the center of the DNA fragment using the 601 positioning sequence[23] (**Fig. 1a** and **Supplementary Fig. 1** online). The 601 sequence provides the thermodynamically most preferred location for the histone octamer on this DNA fragment[23] (data not shown). SNF2h moved both end-positioned and centrally positioned nucleosomes to multiple locations away from the original position (**Fig. 1b**). In contrast, ACF moved the end-positioned nucleosome to a predominantly centered position and did not seem to alter the position of a centered nucleosome (**Fig. 1b**). Nucleosomes were also centered under conditions of limiting ACF (**Supplementary Fig. 2** online), ruling out the possibility that centering results from a second

[1]Department of Biochemistry and Biophysics, University of California, San Francisco, 600 16th Street, San Francisco, California 94158, USA. [2]These authors contributed equally to this work. Correspondence should be addressed to G.J.N. (gnarlikar@biochem.ucsf.edu).

Received 2 October; accepted 24 October; published online 12 November 2006; doi:10.1038/nsmb1170

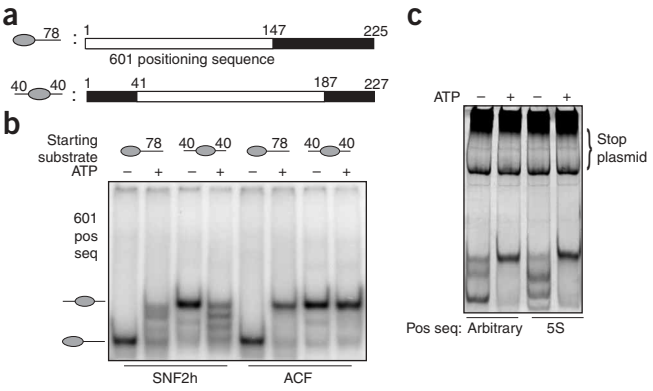

Figure 1 ACF efficiently centers mononucleosomes. (**a**) DNA constructs used to assemble mononucleosomes. (**b**) ^{32}P-labeled nucleosomes, end-positioned or centrally positioned using the 601 sequence, were incubated with SNF2h or ACF, with or without 2 mM ATP (saturating), and processed as described in Methods. On these nondenaturing gels, centrally positioned nucleosomes migrate more slowly than end-positioned nucleosomes[10,12]. (**c**) Unlabeled nucleosomes assembled on either the *Xenopus* 5S sequence or an arbitrary bacterial sequence were incubated with ACF, with or without 2 mM ATP.

molecule of ACF binding DNA that has moved across the nucleosome. Further, ACF centered nucleosomes assembled on the naturally occurring *Xenopus laevis* 5S ribosomal DNA positioning sequence[24] as well as an arbitrary bacterial plasmid sequence with no known positioning ability (**Fig. 1c**). These data show that nucleosome centering by human ACF is sequence independent and, notably, that human ACF can move nucleosomes from the end to the center of DNA, even when the end position is thermodynamically preferred (**Fig. 1b**). This raised the key questions of how ACF overcomes thermodynamic bias to center mononucleosomes and why SNF2h alone cannot do so.

FRET reveals at least one intermediate

Identification of reaction intermediates has provided substantial mechanistic insight into the working of other ATP-utilizing molecular machines such as helicases and kinesin[25]. We reasoned that analogous identification of intermediate steps in the ACF reaction would help us dissect its mechanism. We and others have detected intermediates on a nondenaturing gel or by cross-linking[26,27] (**Supplementary Fig. 3** online). It is possible, however, that these methods do not accurately reflect the transient intermediates formed in solution because of the discontinuous nature of the techniques and, in the case of gel-based methods, interactions with the gel matrix[28]. Therefore, we developed a FRET-based method to visualize the dynamics of nucleosome movement in solution. DNA was end-labeled with Cy3, and a single cysteine substitution at residue 120 of histone H2A was labeled with Cy5 (**Fig. 2a**). The end-positioned nucleosome shown in **Figure 2a** has 78 base pairs (bp) of flanking DNA and has the Cy3 dye on the short DNA end of the nucleosome. We monitored FRET by exciting the nucleosomes at the Cy3 absorption maximum and measuring the Cy3 and Cy5 emissions. Before remodeling, the fluorescence intensity of the Cy3 donor was lower than that of the Cy5 acceptor, and the FRET efficiency was ~100% (**Fig. 2b**, yellow line). This indicated that the two dyes were close together, as expected for an end-positioned nucleosome. After remodeling by human ACF, the fluorescence intensity of the Cy3 donor increased and that of the Cy5 acceptor decreased (**Fig. 2b**, blue line and arrows), indicating that the two dyes had moved apart, as expected for a centered nucleosome.

We then visualized movement of the nucleosome by following the unquenching of Cy3 fluorescence with time. At a saturating ATP concentration (2 mM), most of the ACF reaction was complete within seconds (**Supplementary Fig. 4** online). To reliably capture the remodeling reaction for ACF, we used a subsaturating ATP concentration (4 μM) and found that ACF remodels nucleosomes about six-fold faster than SNF2h alone (**Fig. 2c**), consistent with previous results using gel-based and nuclease footprinting methods[11,12,22].

Next, to determine whether the reaction proceeds through intermediates in which part of the DNA has moved across the histone octamer, we moved the Cy3 dye 17 bp away from the short end of the nucleosome (**Fig. 2d**). For this construct, the FRET efficiency of both the end-positioned and centrally positioned nucleosomes is predicted to be low (<40%). If the DNA gradually moves across the histone octamer during remodeling, the Cy3 and Cy5 dyes will transiently come close together and the FRET efficiency will approach 100% before decreasing again (**Fig. 2d**, bottom). During remodeling with SNF2h (data not shown) and ACF, we saw an increase in FRET followed by a decrease (**Fig. 2e**). This indicated that the Cy3 and Cy5

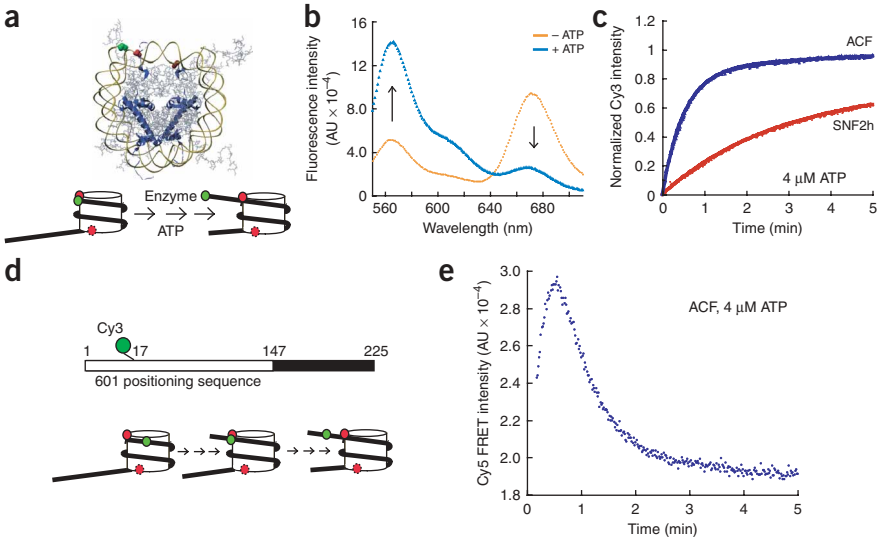

Figure 2 Use of FRET to visualize nucleosome movement in real time. (**a**) Schematic of nucleosome structure[43] with dye attachment sites (top; blue, histone H2A; yellow, DNA; green, Cy3 site; red, two Cy5 sites) and the expected change in dye positions upon remodeling (bottom). (**b**) Nucleosomes in **a** were incubated with ACF for 30 min with (blue) or without (yellow) 2 mM ATP. (**c**) Kinetics of remodeling of the nucleosome in **a** by SNF2h (red) and ACF (blue), as measured by Cy3 unquenching. Rate constants ± s.e.m. (min^{-1}) are as follows: SNF2h, 0.4 ± 0.01; ACF, 2.3 ± 0.3 (see Methods for details of data fitting). (**d**) Schematics of DNA used to detect intermediate in **e** (top) and of potential intermediate (bottom). (**e**) Kinetics of remodeling by ACF of the nucleosome in **d**. AU, arbitrary units.

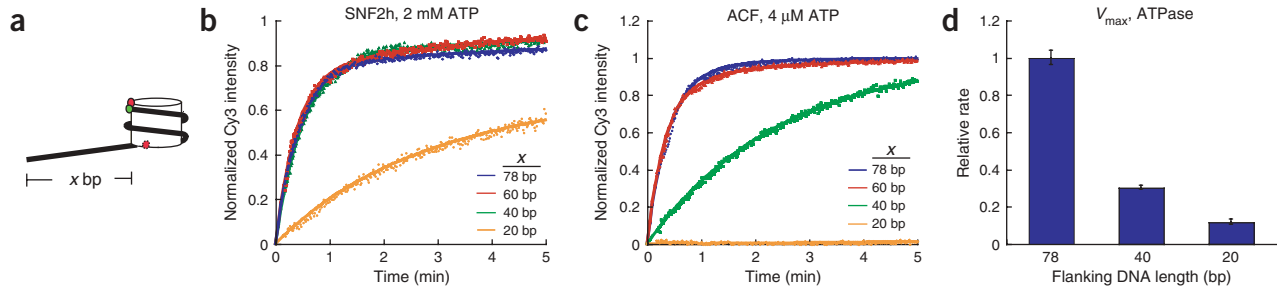

Figure 3 ACF kinetically discriminates between different flanking DNA lengths. (**a**) *x* denotes variable flanking DNA length. (**b**,**c**) Kinetics of remodeling by SNF2h (**b**) and ACF (**c**) as measured by Cy3 donor unquenching. Rate constants ± s.e.m. (min^{-1}) are as follows. SNF2h (2 mM ATP): 78 bp, 2.1 ± 0.3; 60 bp, 2.0 ± 0.6; 40 bp, 1.6 ± 0.3; 20 bp, 0.4 ± 0.04. ACF (4 μM ATP): 78 bp, 2.3 ± 0.3; 60 bp, 2.4 ± 0.6; 40 bp, 0.5 ± 0.1; 20 bp, <0.03. For ACF data at 2 mM ATP, see **Supplementary Fig. 4**. (**d**) Rate of ATP hydrolysis (25 nM ACF, saturating nucleosomes, 4 μM ATP). Error bars represent s.e.m.

dyes transiently came close together and demonstrated the existence of at least one intermediate in which part of the DNA has moved across the octamer. The kinetics are consistent with the presence of the two intermediates detected by gel (**Supplementary Fig. 3**), as both the intermediates are predicted to give a higher FRET signal than the substrate and product. A nucleosome constructed with the arbitrary bacterial DNA sequence was remodeled with similar kinetics (**Supplementary Fig. 5** online), indicating that formation of an intermediate is sequence independent.

Kinetic discrimination between flanking DNA lengths

The above data raised the possibility that human ACF activity may be sensitive to the continuously changing flanking DNA length. Indeed, ISWI complexes contact the core nucleosome as well as the flanking DNA that moves across the histone octamer[26,29–31], and previous studies have suggested that the activity of ISWI complexes is sensitive to flanking DNA length[21,32,33]. To further quantitatively test this hypothesis, we used FRET to measure the remodeling of end-positioned nucleosomes with varying lengths of flanking DNA (**Fig. 3a**). SNF2h remodeled nucleosomes with 78, 60 and 40 bp of flanking DNA with comparable rates, but remodeled nucleosomes with 20 bp of flanking DNA much more slowly (**Fig. 3b**). In contrast, ACF showed the same maximal rate for nucleosomes with flanking DNAs of 78 and 60 bp but showed a progressive decrease in rate as the flanking DNA was further shortened (**Fig. 3c** and **Supplementary Fig. 6** online). A similar DNA-length dependence was observed with nucleosomes assembled on the arbitrary bacterial sequence (**Supplementary Fig. 5**). Notably, these nucleosomes were remodeled at similar rates to the corresponding 601 nucleosomes, even though 601 is predicted to have a much stronger affinity for the histone octamer[23].

It has been suggested previously that ISWI complexes dissociate from the flanking DNA once it gets shortened below a certain limit[20,29]. Therefore, we considered the possibility that nucleosomes with shorter flanking DNA are remodeled more slowly because ACF has reduced affinity for these nucleosomes. To test this, we varied ACF concentration. The remodeling rates for nucleosomes with flanking DNA lengths of 40 and 20 bp, however, were essentially the same for all ACF concentrations between 25 and 100 nM (**Supplementary Fig. 6**), indicating that ACF was saturating and ruling out the above possibility. Thus, human ACF discriminates between different flanking DNA lengths at the level of maximal rates.

Notably, the rate of ATP hydrolysis also decreased with shorter flanking DNA length (**Fig. 3d**). These data are consistent with previous results obtained using a different ISWI enzyme[33]. In ISWI complexes, most of the flanking DNA is bound by the noncatalytic subunits, whereas the ATPase activity is localized solely to the ATPase subunit. Hence, the above data suggest that the noncatalytic subunit ACF1 senses the DNA length and allosterically affects the activity of the ATPase subunit SNF2h.

A model for dynamic nucleosome centering by ACF

The ability of human ACF to kinetically discriminate between different flanking DNA lengths suggested a mechanism for nucleosome

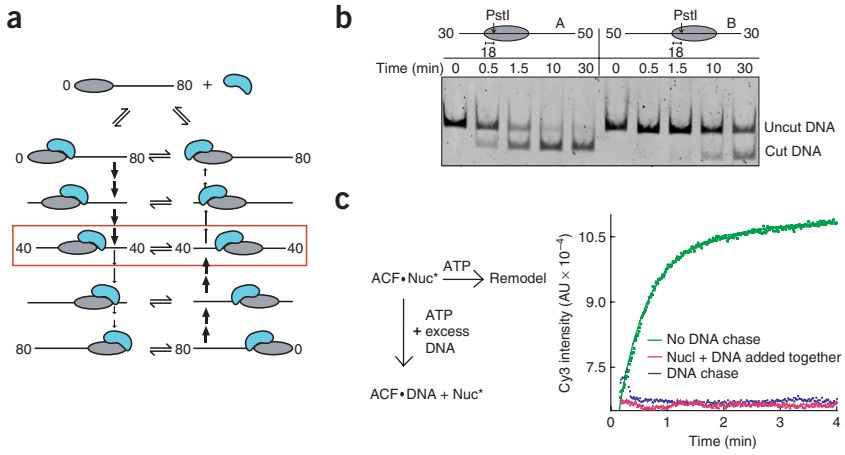

Figure 4 Model for nucleosome centering by ACF. (**a**) ACF creates a dynamic equilibrium between different nucleosome positions such that centered nucleosomes are most highly populated. Thicker arrow indicates faster rate. Blue, ACF; gray, nucleosome. (**b**) One example of data showing that longer flanking DNA is moved in faster than shorter flanking DNA. Kinetics of restriction enzyme accessibility for two different nucleosome constructs (A and B) were monitored. (**c**) ACF falls off of nucleosomes faster than movement of the octamer to the center. Left, schematic of chase experiment; right, the addition of chase substantially decreased the rate of remodeling (blue) of nucleosomes compared to reactions without chase (green). Effectiveness of the chase is demonstrated by results when DNA was added at the same time as nucleosomes (red). Rate constant ± s.e.m. with no chase and 78 bp flanking DNA, 2.3 ± 0.3 min^{-1}.

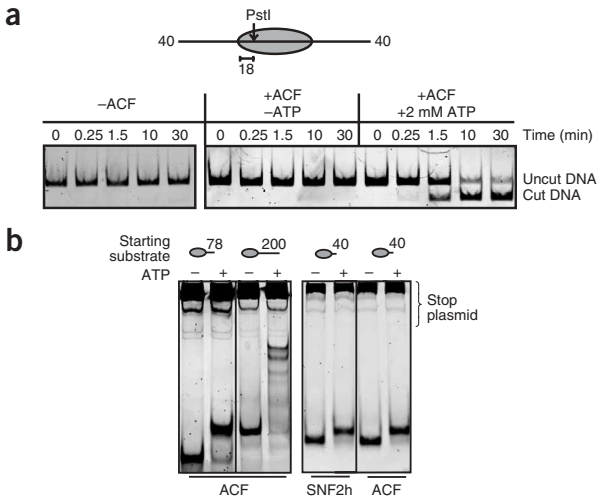

Figure 5 Testing the predictions of the model. (**a**) Centered nucleosomes are moved by ACF. (**b**) Remodeling of unlabeled nucleosomes with 78, 200 or 40 bp of flanking DNA by ACF or SNF2h.

centering (**Fig. 4a**). The model incorporates previous observations that ISWI complexes bind the flanking DNA that is moved across the histone octamer[20,26,29–31]. For simplicity, only one intermediate is shown. In this model, as ACF moves the DNA across the histone octamer, the DNA exiting on the other side becomes an alternative target for ACF binding. If ACF binds the shorter DNA, it can reverse the reaction by moving DNA in the opposite direction. However, this process is slow compared to the forward reaction because of the DNA-length dependence of ACF action (**Fig. 3c**). At every step, ACF can sample and bind either side of the nucleosome, but the longer flanking DNA is moved in faster than the shorter flanking DNA, resulting in a dynamic equilibrium in which the centered product accumulates.

To directly test whether the longer flanking DNA is moved in faster than the shorter flanking DNA, we compared the rate of restriction enzyme accessibility on two nucleosome constructs, one containing a PstI restriction site within the nucleosome near the shorter flanking DNA (nucleosome A) and the other near the longer flanking DNA (nucleosome B) (**Fig. 4b**). We found that the PstI site in nucleosome A was exposed ~17-fold faster than the PstI site in nucleosome B. For the PstI site in nucleosome A to be exposed, the longer flanking DNA has to move across the histone octamer, and vice versa. This indicated that the longer flanking DNA is moved in faster than the shorter flanking DNA (see **Supplementary Fig. 7** online for quantification). Further, for the model to hold, ACF must rapidly fall off and sample both sides of the nucleosome before moving large amounts of flanking DNA across the histone octamer. In a chase experiment using nucleosomal substrates, we found that human ACF falls off from nucleosomes much faster than movement of the octamer to the center (**Fig. 4c**). This is different from previous observations suggesting that remodeling complexes can translocate over long distances on naked DNA[33–36]. It is possible that upon encountering a nucleosome the enzyme falls off more often. A variation of the model assuming human ACF acts as a dimer is described in **Supplementary Figure 8** online[28].

Testing the predictions of the model

Our model predicts that ACF constantly interconverts centered nucleosomes with other positions. To test this, we determined whether a centered nucleosome could be moved by human ACF. We introduced a PstI site 18 bp in from one end of a centered nucleosome (**Fig. 5a**). In the absence of ACF, this site is occluded and cannot be cut by PstI. If ACF does not move centered nucleosomes, then the site will remain occluded. If ACF does move centered nucleosomes, then the site will be exposed and will get cut by PstI. As predicted by our model, the PstI site was exposed upon remodeling, suggesting that ACF moves the nucleosome by at least ~20 bp.

Our model explains why SNF2h cannot center nucleosomes containing ~80 bp of flanking DNA (**Fig. 1b**). This is because SNF2h does not discriminate between flanking DNA lengths until they are shorter than 40 bp. As a result, with ~80 bp of flanking DNA, movement of the octamer toward the center is as fast as movement away from it, and off-center positions are highly populated. Analogously, ACF should not be able to center nucleosomes effectively when the flanking DNA is longer than 120 bp. As expected, when the flanking DNA length was increased to 200 bp, ACF did not reposition the nucleosome to one central position but rather generated multiple positions (**Fig. 5b**, left). Also analogously, both ACF and SNF2h should be able to center nucleosomes with 40 bp of flanking DNA, as both enzymes progressively slow down as the flanking DNA is shortened below 40 bp. As expected, both ACF and SNF2h moved an end-positioned nucleosome containing 40 bp of flanking DNA to a central position (**Fig. 5b**, right). Finally, to quantitatively validate the model, we used the rate constants measured by FRET and a differential-equation solver to model the reaction in **Figure 4a** and confirmed that the output agreed well with our gel-based data (**Supplementary Fig. 3**).

DISCUSSION

Our data explain how human ACF generates arrays of regularly spaced nucleosomes. We show that ACF kinetically discriminates between different flanking DNA lengths and thereby generates a dynamic distribution of nucleosome positions in which nucleosomes with equal DNA on either side accumulate.

By using FRET to visualize ACF-catalyzed movement of DNA in real time, we have identified at least one intermediate in which part of the flanking DNA has moved across the histone octamer. This allowed us to propose a model in which human ACF activity is sensitive to the continuously changing flanking DNA length. A recent model for nucleosome centering posits that ISWI complexes discriminate between different flanking DNA lengths at the level of binding and dissociate from the nucleosome when the flanking DNA decreases below a certain length[20,29]. In contrast, we show that human ACF discriminates between different flanking DNA lengths at the level of maximal rates and thus can center nucleosomes even under saturating ACF concentrations. Our model further explains why ACF can center mononucleosomes on short but not long DNA fragments (**Fig. 5b**).

We propose that in a nucleosome array, adjacent nucleosomes will act analogously to DNA ends in mononucleosomes to define the length of flanking DNA. As a result, ACF action on nucleosome arrays will result in the accumulation of equally spaced nucleosomes. Although our data explain how ACF generates regularly spaced nucleosomes, how this enzyme actually moves the DNA across the histone octamer remains an open question[27,28,30,33].

The insensitivity of ACF to DNA sequence explains how ACF can generate regular nucleosome arrays at several different regions of the genome[3]. Further, it is noteworthy that ACF activity does not seem to be sensitive to the strength of histone-DNA interactions but rather seems to be solely controlled by the length of the flanking. We speculate that this may allow ACF to move nucleosomes away from thermodynamically preferred locations on DNA to help switch between

different chromatin states during development[37]. Indeed, recent data show that the yeast Isw2 complex can reposition nucleosomes away from the default thermodynamically favored location *in vivo*[38].

Together with previous work, the results here indicate that ACF1 modulates the activity of SNF2h in part by changing its sensitivity to flanking DNA length[21]. The noncatalytic subunits in other ISWI complexes may analogously change the sensitivity of the ATPase subunit to flanking DNA length but may differ in their quantitative effects. Further, although ACF activity seems to be independent of DNA sequence, it is possible that both flanking DNA length and sequence modulate the activities of other ISWI complexes. This would result in different final distributions of nucleosome positions depending on the sequence, as observed for the *Drosophila* ISWI protein[12,39].

Because human ACF maintains the remodeled products in a dynamic state, we speculate that to generate a persistent, regularly spaced nucleosome array, ACF needs to act transiently or work with other transcription factors to lock in nucleosome positions. Further, our data imply that ACF would catalyze net movement of nucleosomes in a direction away from barriers such as other nucleosomes or bound factors, as long as the movement is shorter than 60 bp. This is because as soon as 60 bp or more of DNA is available between the barrier and the nucleosome, any ACF-catalyzed movement toward the barrier would be as fast as movement away from it. To maintain directional movement over longer distances, ACF would require the assistance of other DNA-binding factors that bind sites opened up by octamer movement and prevent reversal of octamer movement. This is consistent with previous observations that GAL4 can direct and extend the movement of nucleosomes catalyzed by the *Drosophila* ISWI–containing NURF complex[8], and that the lac repressor can modulate the spacing activity of *Drosophila* ACF[40].

The real-time FRET-based approach described here lays the foundation for the mechanistic study of other factors that regulate chromatin structure. It is clear that several nuclear factors collaborate to regulate chromatin dynamics, and understanding the molecular mechanisms of these factors will be essential for understanding how DNA replication, transcription, recombination and repair are regulated in eukaryotes.

METHODS

Protein purification. Flag-tagged human SNF2h and hemagglutinin (HA)-tagged human ACF1 constructs were individually overexpressed in Sf9 cells using a baculovirus expression system. Nuclear extracts were prepared as described[41]. Before purification, excess HA-ACF1 extract was mixed with Flag-SNF2h extract to ensure ACF complex formation. ACF complex or SNF2h alone was purified using M2-affinity chromatography[41]. The proper stoichiometry of ACF (1:1 molar ratio of ACF1 to SNF2h) subunits was confirmed by SYPRO staining.

Nucleosome assembly. The 601 positioning sequence was modified to contain a PstI site 18 bp in from one end (**Fig. 4b** and **Fig. 5a**). The *Xenopus* 5S positioning sequence was as described[24]. The arbitrary sequence was subjectively chosen from a linker region in the pFastBac1 bacterial plasmid. DNA constructs of different lengths were generated by PCR and gel-purified. DNA fragments were assembled into mononucleosomes with recombinant *Xenopus* histones as described[42]. Cy3-labeled DNA was generated by PCR using end-labeled or internally labeled primers (IDT and IBA). For *Xenopus* 5S–containing and arbitrary positioning sequence–containing nucleosomes, we enriched for end-positioned nucleosomes by glycerol-gradient purification. To obtain ^{32}P-labeled nucleosomes, DNA constructs were prepared by PCR with [α-^{32}P]dATP. Positions of mononucleosomes were mapped as described[10,18].

To generate octamers with labeled H2A, a unique cysteine was engineered at residue 120 and subsequently labeled with Cy5 maleimide in a buffer containing 20 mM Tris (pH 7.0), 7 M guanidinium hydrochloric acid and 5 mM EDTA. Unreacted dye was removed using a microcon concentrator. The labeled histone was refolded with the other histones as described[42] to generate octamers. Labeling efficiency was estimated to be ~60%–70%. As each octamer contains two copies of H2A, two Cy5 dyes can be incorporated per nucleosome. On the basis of the crystal structure[43], the two Cy5 dyes are predicted to be 2 and 6 nm away from Cy3, respectively. The Förster radius for Cy3 and Cy5 is ~5 nm, so only the Cy5 dye that is 2 nm away from Cy3 will act as an efficient acceptor. FRET efficiency was calculated using the following equations[44].

$$F^{\mathrm{FRET}}_{670,520} = F^{\mathrm{DA}}_{670,520} - (F^{\mathrm{DA}}_{565,520} \cdot F^{\mathrm{D}}_{670,520}/F^{\mathrm{D}}_{565,520}) - (F^{\mathrm{DA}}_{670,610} \cdot F^{\mathrm{A}}_{670,520}/F^{\mathrm{A}}_{670,610})$$

$$E = F^{\mathrm{FRET}}_{670,520} \cdot \varepsilon^{\mathrm{A}}_{610}/F^{\mathrm{FRET}}_{670,520} \cdot \varepsilon^{\mathrm{D}}_{520} \cdot d$$

where F is the fluorescence signal, at the emission and excitation wavelengths indicated by subscripts, from the dyes indicated by superscripts (with D and A denoting Cy3 and Cy5, respectively); E is the FRET efficiency; ε are extinction coefficients such that $\varepsilon^{\mathrm{D}}_{520} = 150{,}000\ \mathrm{M}^{-1}\ \mathrm{cm}^{-1}$ and $\varepsilon^{\mathrm{A}}_{610} = 80{,}000\ \mathrm{M}^{-1}\ \mathrm{cm}^{-1}$; and d is the efficiency of labeling (~0.6–0.7).

$$E = R^6/(R^6 + r^6)$$

where R is the Förster radius (~5 nm) and r is the distance between Cy3 and Cy5.

Molecular graphics images were produced using the Chimera package from the Resource for Biocomputing, Visualization and Informatics at the University of California, San Francisco (http://www.cgl.ucsf.edu/chimera). Primer sequences are available upon request.

Gel mobility shift experiments. All experiments described below were performed at 30 °C in reaction buffer (12 mM HEPES (pH 7.9), 4 mM Tris (pH 7.5), 60 mM KCl, 3 mM $MgCl_2$, 0.32 mM EDTA, 12% (v/v) glycerol, 0.02% (v/v) Nonidet P40, 0.4 mg ml^{-1} Flag peptide). SNF2h (300 nM) or 25–50 nM ACF was incubated with 20 nM nucleosomes in the presence or absence of 2 mM ATP for 30 min, unless otherwise noted. ^{32}P-labeled nucleosomes were used at 1 nM final concentration. For experiments with limiting ACF, 20 nM nucleosomes were mixed with 5 nM ACF. Reactions were stopped with 2 stop buffer (115 mM ADP, 0.8 mg ml^{-1} unrelated stop plasmid DNA) to compete off the enzyme and run on a 0.5 TBE non-denaturing 5% (v/v) polyacrylamide gel. ^{32}P-containing gels were dried and exposed on a phosphorimager screen. Unlabeled nucleosome gels were stained with SYBR Gold. All gels were scanned on a Typhoon Variable Mode Imager.

FRET-based experiments. Steady-state fluorescence was measured on an ISS K2 fluorometer. Samples were excited at 520 nm with a 400-nm cutoff filter and emission spectra collected from 540 to 710 nm with a 495-nm cutoff filter. For kinetic measurements, samples were excited at 520 nm and spectra collected at Cy3 or Cy5 peak intensity, 565 or 668 nm, respectively. Reactions were initiated by addition of ATP and contained 5 nM nucleosomes, 300 nM SNF2h or 25 nM ACF, and either 4 μM or 2 mM ATP, as noted in the figures. Data were collected for at least 10 min, sampled once per second. For the nucleosomes used in **Figure 2c** and **Figure 3**, we often see a fast phase in which most of the FRET signal decreases (~90%) followed by a second slow phase. The second slow phase is the result of a small fraction of the nucleosomes that react about ten-fold more slowly. The data were fit to two exponentials using Kaleidagraph (Synergy Software). The rate constants reported in the figure legends are for the fast phase. For chase experiments (**Fig. 5**), excess, saturating ACF (25 nM) was allowed to bind nucleosomes (5 nM). DNA in molar excess of ACF was then added as a chase at the same time as ATP (final concentration of 2 mM ATP and 2.4 mg ml^{-1} unrelated 3 kbp plasmid DNA).

ATPase reactions. Reactions containing 5 nM (**Supplementary Fig. 6**) or 25 nM ACF (**Fig. 3**) and varying amounts of nucleosomes were initiated by the addition of 4 μM ATP containing trace amounts of [γ-^{32}P]ATP. Reactions were quenched, processed and quantified as described[45].

Restriction enzyme accessibility reactions. Nucleosomes (5 nM) were incubated with 2 units μl^{-1} PstI in the presence or absence of 25 nM ACF and 2 mM ATP. Reactions were quenched, processed and quantified as described[45].

Requests for materials. gnarlikar@biochem.ucsf.edu.

Note: Supplementary information is available on the Nature Structural & Molecular Biology website.

ACKNOWLEDGMENTS

We thank J. Widom (Northwestern University) for the 601 plasmid, J.J. Hayes (University of Rochester Medical Center) for the 5S plasmid, H.-Y. Fan and R.E. Kingston (Harvard Medical School) for SNF2h and ACF1 constructs, R.D. Mullins (University of California, San Francisco) for use of the fluorometer, K. Ashrafi, H.-Y. Fan, J.T. Kadonaga, B. Panning, A.K. Srivastava, J.S. Weissman, J. Widom, C. Wu and K.R. Yamamoto for helpful comments on the manuscript and members of the Narlikar lab for technical advice and discussion. J.G.Y. is supported by a US National Science Foundation Graduate Research Fellowship. This work was supported in part by a grant from the US National Institutes of Health (to G.J.N.).

AUTHOR CONTRIBUTIONS

J.G.Y., T.S.M. and G.J.N. designed the experiments, J.G.Y. and T.S.M. did the experiments and analyzed the data, E.S. made reagents for the experiments and J.G.Y. and G.J.N. interpreted the data and wrote the manuscript.

COMPETING INTERESTS STATEMENT

The authors declare that they have no competing financial interests.

Published online at http://www.nature.com/nsmb/
Reprints and permissions information is available online at http://npg.nature.com/reprintsandpermissions/

1. Huisinga, K.L., Brower-Toland, B. & Elgin, S.C. The contradictory definitions of heterochromatin: transcription and silencing. *Chromosoma* **115**, 110–122 (2006).
2. Sun, F.L., Cuaycong, M.H. & Elgin, S.C. Long-range nucleosome ordering is associated with gene silencing in *Drosophila melanogaster* pericentric heterochromatin. *Mol. Cell. Biol.* **21**, 2867–2879 (2001).
3. Fyodorov, D.V., Blower, M.D., Karpen, G.H. & Kadonaga, J.T. Acf1 confers unique activities to ACF/CHRAC and promotes the formation rather than disruption of chromatin *in vivo*. *Genes Dev.* **18**, 170–183 (2004).
4. Ito, T., Bulger, M., Pazin, M.J., Kobayashi, R. & Kadonaga, J.T. ACF, an ISWI-containing and ATP-utilizing chromatin assembly and remodeling factor. *Cell* **90**, 145–155 (1997).
5. Deuring, R. *et al.* The ISWI chromatin-remodeling protein is required for gene expression and the maintenance of higher order chromatin structure *in vivo*. *Mol. Cell* **5**, 355–365 (2000).
6. Fazzio, T.G. *et al.* Widespread collaboration of Isw2 and Sin3-Rpd3 chromatin remodeling complexes in transcriptional repression. *Mol. Cell. Biol.* **21**, 6450–6460 (2001).
7. Goldmark, J.P., Fazzio, T.G., Estep, P.W., Church, G.M. & Tsukiyama, T. The Isw2 chromatin remodeling complex represses early meiotic genes upon recruitment by Ume6p. *Cell* **103**, 423–433 (2000).
8. Kang, J.G., Hamiche, A. & Wu, C. GAL4 directs nucleosome sliding induced by NURF. *EMBO J.* **21**, 1406–1413 (2002).
9. Mizuguchi, G., Tsukiyama, T., Wisniewski, J. & Wu, C. Role of nucleosome remodeling factor NURF in transcriptional activation of chromatin. *Mol. Cell* **1**, 141–150 (1997).
10. Hamiche, A., Sandaltzopoulos, R., Gdula, D.A. & Wu, C. ATP-dependent histone octamer sliding mediated by the chromatin remodeling complex NURF. *Cell* **97**, 833–842 (1999).
11. Eberharter, A. *et al.* Acf1, the largest subunit of CHRAC, regulates ISWI-induced nucleosome remodeling. *EMBO J.* **20**, 3781–3788 (2001).
12. Langst, G., Bonte, E.J., Corona, D.F. & Becker, P.B. Nucleosome movement by CHRAC and ISWI without disruption or trans-displacement of the histone octamer. *Cell* **97**, 843–852 (1999).
13. Tsukiyama, T., Palmer, J., Landel, C.C., Shiloach, J. & Wu, C. Characterization of the imitation switch subfamily of ATP-dependent chromatin-remodeling factors in *Saccharomyces cerevisiae*. *Genes Dev.* **13**, 686–697 (1999).
14. Varga-Weisz, P.D. *et al.* Chromatin-remodeling factor CHRAC contains the ATPases ISWI and topoisomerase II. *Nature* **388**, 598–602 (1997).
15. Corona, D.F. *et al.* ISWI is an ATP-dependent nucleosome remodeling factor. *Mol. Cell* **3**, 239–245 (1999).
16. Poot, R.A. *et al.* HuCHRAC, a human ISWI chromatin remodeling complex contains hACF1 and two novel histone-fold proteins. *EMBO J.* **19**, 3377–3387 (2000).
17. LeRoy, G., Orphanides, G., Lane, W.S. & Reinberg, D. Requirement of RSF and FACT for transcription of chromatin templates in vitro. *Science* **282**, 1900–1904 (1998).
18. Fan, H.Y., He, X., Kingston, R.E. & Narlikar, G.J. Distinct strategies to make nucleosomal DNA accessible. *Mol. Cell* **11**, 1311–1322 (2003).
19. Bochar, D.A. *et al.* A family of chromatin remodeling factors related to Williams syndrome transcription factor. *Proc. Natl. Acad. Sci. USA* **97**, 1038–1043 (2000).
20. Stockdale, C., Flaus, A., Ferreira, H. & Owen-Hughes, T. Analysis of nucleosome repositioning by yeast ISWI and Chd1 chromatin remodeling complexes. *J. Biol. Chem.* **281**, 16279–16288 (2006).
21. He, X., Narlikar, G.J., Fan, H.Y. & Kingston, R.E. HAcf1 alters the remodeling strategy of SNF2H. *J. Biol. Chem.* **281**, 28636–28647 (2006).
22. Ito, T. *et al.* ACF consists of two subunits, Acf1 and ISWI, that function cooperatively in the ATP-dependent catalysis of chromatin assembly. *Genes Dev.* **13**, 1529–1539 (1999).
23. Lowary, P.T. & Widom, J. New DNA sequence rules for high affinity binding to histone octamer and sequence-directed nucleosome positioning. *J. Mol. Biol.* **276**, 19–42 (1998).
24. Wolffe, A.P. & Hayes, J.J. Transcription factor interaction with model nucleosomal templates. *Methods Mol. Genet.* **2**, 314–330 (1993).
25. Lohman, T.M., Thorn, K. & Vale, R.D. Staying on track: common features of DNA helicases and microtubule motors. *Cell* **93**, 9–12 (1998).
26. Schwanbeck, R., Xiao, H. & Wu, C. Spatial contacts and nucleosome step movements induced by the NURF chromatin remodeling complex. *J. Biol. Chem.* **279**, 39933–39941 (2004).
27. Zofall, M., Persinger, J., Kassabov, S.R. & Bartholomew, B. Chromatin remodeling by ISW2 and SWI/SNF requires DNA translocation inside the nucleosome. *Nat. Struct. Mol. Biol.* **13**, 339–346 (2006).
28. Strohner, R. *et al.* A 'loop recapture' mechanism for ACF-dependent nucleosome remodeling. *Nat. Struct. Mol. Biol.* **12**, 683–690 (2005).
29. Kagalwala, M.N., Glaus, B.J., Dang, W., Zofall, M. & Bartholomew, B. Topography of the ISW2-nucleosome complex: insights into nucleosome spacing and chromatin remodeling. *EMBO J.* **23**, 2092–2104 (2004).
30. Langst, G. & Becker, P.B. ISWI induces nucleosome sliding on nicked DNA. *Mol. Cell* **8**, 1085–1092 (2001).
31. Fazzio, T.G. & Tsukiyama, T. Chromatin remodeling *in vivo*: evidence for a nucleosome sliding mechanism. *Mol. Cell* **12**, 1333–1340 (2003).
32. Zofall, M., Persinger, J. & Bartholomew, B. Functional role of extranucleosomal DNA and the entry site of the nucleosome in chromatin remodeling by ISW2. *Mol. Cell. Biol.* **24**, 10047–10057 (2004).
33. Whitehouse, I., Stockdale, C., Flaus, A., Szczelkun, M.D. & Owen-Hughes, T. Evidence for DNA translocation by the ISWI chromatin-remodeling enzyme. *Mol. Cell. Biol.* **23**, 1935–1945 (2003).
34. Saha, A., Wittmeyer, J. & Cairns, B.R. Chromatin remodeling by RSC involves ATP-dependent DNA translocation. *Genes Dev.* **16**, 2120–2134 (2002).
35. Amitani, I., Baskin, R.J. & Kowalczykowski, S.C. Visualization of Rad54, a chromatin remodeling protein, translocating on single DNA molecules. *Mol. Cell* **23**, 143–148 (2006).
36. Lia, G. *et al.* Direct observation of DNA distortion by the RSC complex. *Mol. Cell* **21**, 417–425 (2006).
37. Segal, E. *et al.* A genomic code for nucleosome positioning. *Nature* **442**, 772–778 (2006).
38. Whitehouse, I. & Tsukiyama, T. Antagonistic forces that position nucleosomes *in vivo*. *Nat. Struct. Mol. Biol.* **13**, 633–640 (2006).
39. Flaus, A. & Owen-Hughes, T. Dynamic properties of nucleosomes during thermal and ATP-driven mobilization. *Mol. Cell. Biol.* **23**, 7767–7779 (2003).
40. Levenstein, M.E. & Kadonaga, J.T. Biochemical analysis of chromatin containing recombinant *Drosophila* core histones. *J. Biol. Chem.* **277**, 8749–8754 (2002).
41. Aalfs, J.D., Narlikar, G.J. & Kingston, R.E. Functional differences between the human ATP-dependent nucleosome remodeling proteins BRG1 and SNF2H. *J. Biol. Chem.* **276**, 34270–34278 (2001).
42. Luger, K., Rechsteiner, T.J. & Richmond, T.J. Preparation of nucleosome core particle from recombinant histones. *Methods Enzymol.* **304**, 3–19 (1999).
43. Davey, C.A., Sargent, D.F., Luger, K., Maeder, A.W. & Richmond, T.J. Solvent mediated interactions in the structure of the nucleosome core particle at 1.9 Å resolution. *J. Mol. Biol.* **319**, 1097–1113 (2002).
44. Mukhopadhyay, J. *et al.* Translocation of sigma(70) with RNA polymerase during transcription: fluorescence resonance energy transfer assay for movement relative to DNA. *Cell* **106**, 453–463 (2001).
45. Narlikar, G.J., Phelan, M.L. & Kingston, R.E. Generation and interconversion of multiple distinct nucleosomal states as a mechanism for catalyzing chromatin fluidity. *Mol. Cell* **8**, 1219–1230 (2001).